Multiple non-auditory cortical regions innervate the auditory midbrain

Abbreviated title: Cortical inputs to the auditory midbrain

Bas MJ Olthof*, Adrian Rees[#] and Sarah E Gartside[#]

Institute of Neuroscience, Newcastle University, Newcastle upon Tyne, NE2 4HH, UK

*Bas Olthof
bas.olthof@ncl.ac.uk

[#]Joint senior authors

Number of pages 29

Number of figures 10

Abstract words 182

Introduction 619

Discussion 1487

Conflict of Interest
The authors have no conflicts of interests.

Acknowledgements:

This work was supported by the BBSRC (Grant BB/P003249/1 to A.R. and S.E.G.). We thank the Newcastle University BioImaging Unit for their support and assistance in performing the microscopy, Andrew Trevelyan for advice on tracer injection and Michael Schmid for comments on an earlier version of the manuscript.

LIST OF ABBREVIATIONS

AC, auditory cortex; **AI**, agranular insular cortex; **Au1**, primary auditory cortex; **AuD**, secondary auditory cortex dorsal zone; **AuV**, secondary auditory cortex, ventral zone; **Cg1**, cingulate cortex area 1; **Cg2**, cingulate cortex area 2; **Den**, dorsal endopiriform nucleus; **DI**, dysgranular insular cortex; **DP**, dorsal peduncular cortex; **DZ**, primary somatosensory cortex dorsal zone; **Ect**, ectorhinal cortex; **GI**, granular insular cortex; **IC**, inferior colliculus; **ICc**, central nucleus of inferior colliculus; **ICd**, dorsal cortex of inferior colliculus; **ICl**, lateral cortex of inferior colliculus; **IL**, infralimbic cortex; **LO**, lateral orbital cortex; **M1**, primary motor cortex; **M2**, secondary motor cortex; **MO**, medial orbital cortex; **nNOS**, nitric oxide synthase; **PFC**, prefrontal cortex; **Prh**, perirhinal cortex; **PrL**, prelimbic cortex; **RSA**, retrosplenial agranular cortex; **RSG**, retrosplenial granular cortex; **RSGb**, retrosplenial granular b cortex; **S1**, primary somatosensory cortex; **S1BF**, primary somatosensory barrel cortex; **S1Tr**, primary somatosensory cortex trunk region; **S2**, secondary somatosensory cortex; **TeA**, temporal association cortex; **V1B**, primary visual cortex, binocular area; **V1M**, primary visual cortex, monocular area; **V2L**, secondary visual cortex, lateral area; **V2M**, secondary visual cortex, mediolateral area; **VC**, visual cortex; **VO**, ventral orbital cortex.

ABSTRACT

Our perceptual experience of sound depends on the integration of multiple sensory and cognitive domains, but the networks sub-serving this integration are unclear. Connections linking different cortical domains have been described, however we do not know the extent to which connections also exist between multiple cortical domains and subcortical structures. Retrograde tracing in adult male rats (*Rattus norvegicus*) revealed that the inferior colliculus – the auditory midbrain - not only receives dense descending projections as previously established from the auditory cortex, but also the visual, somatosensory, motor, and prefrontal cortices. While all these descending connections are bilateral, those from sensory areas show a more pronounced ipsilateral dominance than those from motor and prefrontal cortices. Injections of anterograde tracers into the cortical areas identified by retrograde tracing confirmed those findings and revealed cortical fibres terminating in all three subdivisions of the inferior colliculus. Immunolabelling showed that the terminals target both GABAergic inhibitory and putative glutamatergic excitatory neurons. These findings demonstrate that auditory perception and behaviour is served by a network that includes extensive descending connections to the midbrain from sensory, behavioural, and executive cortices.

SIGNIFICANCE STATEMENT

Making sense of what we hear not only depends on the analysis of sound, but also on information from other senses as well as the brain's predictions about the properties and significance of the sound. Previous work suggested that this interplay between the senses and the predictions from higher cognitive centres, occurs within the cerebral cortex. By tracing neural connections in rat, we show that the inferior colliculus – the subcortical, midbrain centre for hearing - receives extensive connections from areas of the cerebral cortex concerned with vision, touch, movement, and cognitive function, in addition to areas representing hearing. These findings demonstrate that wide-ranging cortical feedback operates at an earlier stage of the hearing pathway than previously recognised.

INTRODUCTION

Sensory processing has traditionally been viewed as the centripetal flow of information from a sense organ to a modality-specific region of the cerebral cortex. This view is now being revaluated on two grounds. First, evidence for extensive feedback connections from higher levels to earlier stages in the processing hierarchy demonstrates the flow of information is not one way. Such top-down processing is in keeping with a growing appreciation that perception involves the interaction between predictions or expectations based on prior experience and incoming sensory information (Rao and Ballard, 1999; Friston, 2005; Bastos et al., 2012). A second challenge to the traditional view of sensory processing, is recent evidence that areas of cortex previously considered to be exclusively unimodal, including so called primary regions, can respond to stimuli of other modalities (Kayser and Logothetis, 2007).

Top-down and cross-modal sensory interactions have been most extensively explored in the cerebral cortex, but the organisation of the auditory system, with its many subcortical centres, means that such interactions could potentially occur much earlier in the pathway. The inferior colliculus (IC) - the midbrain auditory centre- receives extensive top-down input from the auditory cortex (Diamond et al., 1969; Beyerl, 1978; Andersen et al., 1980; Saldana et al., 1996; Winer et al., 1998; Budinger et al., 2000; Bajo and Moore, 2005; Coomes et al., 2005; Bajo et al., 2007). Cortico-collicular projections to the dorsal and lateral cortices of the IC (IC_D and IC_L, respectively) are known to be particularly dense, but connections to the central nucleus (IC_C), the main recipient of afferent input from lower level brainstem centres, have also been reported in rat (Feliciano and Potashner, 1995; Saldana et al., 1996) and other species (Budinger et al., 2000; Bajo et al., 2007). These cortico-collicular connections mediate both short and long term plasticity that influences the response properties of neurons in the IC to sounds (Gao and Suga, 2000; Suga and Ma, 2003; Bajo et al., 2010; Bajo and King, 2013).

While research on cortico-collicular connections has focussed almost exclusively on those originating from the auditory cortex, an earlier anatomical study, Cooper and Young (1976), conducted before

the advent of modern tracers, suggested that inputs to the IC might originate from more diverse cortical sources. Cooper and Young (1976) found degenerating fibres in the IC following lesions to the visual, 'somaesthetic' (somatosensory) and motor cortices, suggestive of cortico-collicular inputs from these non-auditory cortices. Surprisingly, despite this evidence, the intriguing possibility that the IC receives extensive inputs from cortical areas other than those sub-serving audition, has not been addressed systematically. The concept of cortical feedback from non-auditory regions to the IC would be congruent with evidence for non-auditory afferent feed-forward sensory inputs that terminate in the cortical subdivisions of the IC. These include connections from the somatosensory dorsal column and spinal trigeminal nuclei to ICL (Aitkin et al., 1978; Aitkin et al., 1981; Jain and Shore, 2006), and visual inputs from the retina (Itaya and Van Hoesen, 1982; Yamauchi and Yamadori, 1982) and other potential sources in the brainstem including the superior colliculus (Adams, 1980; Coleman and Clerici, 1987).

Here we use retrograde and anterograde tracing to identify definitively which regions of the cerebral cortex project to the IC, and used immunohistochemistry to define the neuronal targets of these connections. We demonstrate that extensive projections from sensory, motor, and executive cortices innervate all subdivisions of the IC. These findings show that our understanding of perceptual processing, and specifically the contribution of the auditory midbrain, must take account of these several and diverse sources of top-down cortical input. We speculate that such feedback mechanisms may provide multisystem prediction and feedback signals that are essential for an individual to make sense of, and respond to, the auditory world.

METHODS

Animals

Experiments were performed in accordance with the terms and conditions of a license (PPL 60/3934) issued by the UK Home Office under the Animals (Scientific Procedures) Act 1986 and with the

approval of the Local Ethical Review committee of Newcastle University. Male Lister-hooded rats (*Rattus norvegicus*, 250-350 g, age 9-15 weeks) were obtained from Charles River and housed in the Newcastle University Comparative Biology Centre in keeping with the ARRIVE (Animal Research: Reporting of In Vivo Experiments) guidelines. Rats were acclimatised for at least five days before use and were maintained in an enriched environment under a 12 hour light:dark cycle (lights on 7 am - 7 pm) with access to food and water ad libitum.

Surgical procedures

Animals were heavily sedated with ketamine/medetomidine (≈15 / 0.2 mg/kg, i.p.) and the scalp was shaved. Local anaesthetic cream (Emla™) was applied to the nose and a paediatric nasogastric tube was inserted into one nostril for the delivery of isoflurane in O_2. The concentration of isoflurane was adjusted (1-4 % in ≈0.1 litres/min O_2) to provide a surgical plane of anaesthesia throughout. Animals were placed in a stereotaxic frame using atraumatic ear bars (David Kopf) with the tooth bar set at -0.3 mm (flat skull position). Body temperature was measured with a rectal probe and maintained at 37°C with a homeothermic blanket (Harvard Instruments™). A midline incision was made in the scalp and the periosteum was removed to reveal the skull.

For **retrograde tracing** experiments (n=8), a craniotomy was performed over both ICs (co-ordinates from Bregma AP: -8.5 mm, ML: ± 2.0 mm) leaving a bridge of bone in the midline. Retrobead™ latex nanoparticles (Lumafluor) were injected using a Nanoject™ programmable injector (Drummond Scientific) fitted with a borosilicate glass capillary pipette (1.14 mm OD, 0.53 mm ID, Drummond Scientific) which had been pulled to a fine tip and broken back to allow filling from the tip. Pipettes were preloaded with aloe vera and a small volume of Retrobeads at the tip end. Red Retrobeads were injected into the right IC and green Retrobeads into the left IC. In each case the pipette was initially lowered in the ICc to a depth of -4.5 mm from the brain surface and 200 nl Retrobeads were injected over a period of 2 minutes. The pipette was left *in situ* for 2 min before being raised to -3.3 mm where

a further 200 nl was injected, and then to -2.3 mm where a final 200 nl injection was made. To reduce the likelihood of the injection being drawn upwards through the tissue following the final injection, the pipette was left in place for 5 minutes before it was removed.

For **anterograde tracing** experiments, TRITC- or fluorescein -labelled dextran was injected into either one or two cortical regions (n=10; Table 1). A glass capillary pipette (1.14 mm OD, 0.53 mm ID, Drummond Scientific) pre-loaded with TRITC- or fluorescein-labelled dextran (10,000 m.wt, D1816 and D1821, Invitrogen, 10mg/ml in sterile 0.9 % saline) was fitted to the Nanoject injector. Injections (200 nl/site x 2 minutes) were made at two or three positions in each region. Cortical regions targeted were as follows: **auditory cortex** (craniotomy at AP:-5.2, ML: 4.8 mm, injector angled at 30-20° away from the midline, injection sites corresponding to AP: -5.2, ML: 7.4, DV: -5.6 mm; AP: -5.2, ML: 6.8, DV: -4.2 mm; and AP: -5.2, ML: 5.8, DV: -1.6 mm); **prefrontal cortex** (AP: +3.2, ML: 0.5, DV: -4.3, -2.8, and -1.6 mm); **motor cortex** (injections at AP: +3.2, ML: 1.0, DV: -1.0 mm and AP: +3.2, ML: -1.7, DV: -2.2 mm); **somatosensory cortex** (AP: +2.1, ML: 5.0, DV -1.9 and -1.0 mm); and **visual cortex** (AP: -8.0, ML: 2.5, DV: -0.8mm, and AP: -8.0, ML: 4.1, DV: 1.30 mm, and AP: -8.0, ML: 5.1, DV: -1.0 mm). TRITC-labelled dextran (red) was always injected into the right hemisphere and fluorescein-labelled dextran (green) was injected into the left hemisphere. Following injection, the pipette was left in place for 5 min to minimise the spread of the injection.

Towards the end of the surgical procedure, animals received an injection of meloxicam (15 µg, s.c.) to provide analgesia during recovery. When injections were complete, the scalp wound was stitched using Vicryl™ 4.0 suture (Ethicon) and local anaesthetic cream (Emla™) was applied to the wound. Animals were allowed to recover from the anaesthetic in a warm environment and were then returned to their home cage and normal housing conditions. The next morning, a second dose of meloxicam (15 µg, s.c.) was administered to provide on-going analgesia.

Tissue collection and processing

Between 48 and 60 hours following Retrobead injection, or 7 to 8 days following injection of dextran, animals were deeply anaesthetized with pentobarbital (≈400mg/kg) and transcardially perfused with ≈100ml heparinised 0.1 M phosphate buffered saline (PBS, composition (mM):-NaCl: 66, Na_2HPO_4: 16, KH_2PO_4 3.8) followed by ≈ 100 ml 4% paraformaldehyde in PBS (PFA). The brain was removed, post-fixed overnight in 4 % PFA, and then cryoprotected in 30 % sucrose in PBS. Cryoprotected brains were stored at -80 °C until sectioning.

For **retrograde tracing** experiments, the brain was sectioned on a cryostat from the cerebellum to the olfactory bulb. Coronal sections (30 or 40 µm) were collected onto gelatine subbed slides, air dried, and stored at -20 °C. Before imaging, slides were dipped in DAPI (1 µg/ml, 5 min), air dried and cover-slipped with Fluoroshield™ mounting medium (Sigma-Aldrich).

For **anterograde tracing** experiments, the cortical injection sites and the IC were sectioned. Coronal sections (30 µm) were cut on a rotary microtome and collected into antifreeze solution (30 % ethylene glycol, 30 % sucrose, 1 % polyvinyl pyrrolidone (PVP)-40 in PBS) (Watson et al., 1986) and stored at -20 °C. Sections from the injection sites and the IC were mounted on glass slides, dipped in DAPI (1 µg/ml, 5 min), rinsed and cover-slipped with Fluoroshield™ mounting medium (Sigma-Aldrich).

One mid rostro-caudal IC section from each animal was immunolabelled for GABA (rabbit anti-GABA antibody 1:1000, Sigma-Aldrich Cat# A2052, RRID:AB_477652), and the neuronal marker NeuN (mouse anti-NeuN antibody 1:1000, Merck Millipore Cat# MAB377, RRID: RRID:AB_2298772). A second section was immunolabelled for nitric oxide synthase (nNOS; rabbit anti-nNOS (1:3000, Sigma-Aldrich Cat# N7280, RRID:AB_260796) to identify the subdivisions of the IC (see below). Sections were washed with PBS (3x10 min), incubated in 1 % $NaBH_4$ for antigen retrieval (30 min), and washed in PBS (3x10 min) before being incubated (4 h at room temperature followed by overnight at 8 °C) in a mixture containing the primary antibodies made up in a block buffer comprising 1 % bovine serum albumin (Sigma-Aldrich), 0.1 % porcine gelatine (BDH), 50 mM glycine (Fisher) in PBS. Sections were washed again (3x10 min PBS) before incubation (2 h at room temperature) with a mixture of

AlexaFluor 488 or 568 goat anti-rabbit secondary (1:500, Life Technologies) and biotinylated horse anti-mouse secondary (1:500, Vector labs) in 5 % normal goat serum (Sigma-Aldrich) in PBS. Sections were washed in PBS (3x10 min) and incubated with Cy5 streptavidin (1:500, Life Technologies) in PBS (1 h at room temperature). Finally sections were washed in PBS (10 min), incubated in DAPI (1 µg/ml, 10 min), washed again in PBS (10 min) and dipped in distilled water before mounting on plain glass slides. Slides were cover-slipped with Fluoroshield (Sigma-Aldrich).

Imaging

For **retrograde tracing** experiments, first the injection sites were examined to verify proper placement of the injection and to determine the extent of local spread of the tracer. Only labelling from appropriately placed injections (15/16) was further examined. Next every third slide through the brain was inspected for the presence of red and green fluorescent Retrobeads on a wide field microscope (Nikon NiE equipped with an Andor Zyla 5.2. camera). Detailed notes of areas with retrogradely labelled cells were made on a copy of the Brain Atlas in Stereotaxic Co-ordinates (Paxinos and Watson, 1998).

Three animals in which the injection of Retrobeads was of very similar size and centred within the ICc at a midrostro-caudal level were chosen for quantitative analysis. For these three animals, low power confocal mosaic images of cortical regions and the IC injection sites were acquired with a Zeiss AxioObserver Z1, with a LSM800 confocal scan head, fitted with a motorised stage using a 20x air objective (0.8 numerical aperture (NA), 0.52 µs pixel dwell time, X-Y dimension 1024x1024, bit depth 8 with linear look-up tables (LUTs)). The images were examined and cells containing fluorescent beads were manually tagged in FIJI/ImageJ (Schindelin et al., 2012) using the Cell Counter plugin. Since the red beads were much more easily distinguished than the green beads, for quantification purposes, we counted only cells containing red beads in the cortices both ipsi-and contralateral to the injection site.

For **anterograde tracing experiments**, low-power confocal mosaic images (x20 air, 0.8 NA, 1024 pixels in the X–Y dimension, 0.52 µs pixel dwell time, bit depth 8 with linear LUTs) of the injection sites, were first acquired from DAPI labelled sections to verify the proper placement of injections. Next, confocal mosaic images (x 40 oil, 1.3 NA, 1024 pixels in the X–Y dimension, 6.06 µs pixel dwell time, bit depth 16 with linear LUTs) of the whole IC at a mid-rostro-caudal level in the section immunolabelled for nNOS were acquired, and the presence of red and green dextran in the three subdivisions of the IC (ICC, ICD and ICL) was examined. The borders of these subdivisions were delineated by the distribution of labelling for nNOS. ICD and ICL are characterised by neurons with cytoplasmic labelling for nNOS, whereas, the ICC contains few neurons that label cytoplasmically (Coote and Rees 2008, Olthof et al 2019). This difference makes the borders between the subdivisions easy to distinguish (Fig 7a). Since TRITC-dextran was more easily visualised and quantified than fluorescein-dextran, in six cases we examined only the distribution of red dextran in both hemispheres after injection into the right hemisphere (Fig. 6a-d). In two cases (one visual cortex injection and one somatosensory cortex injection, Fig. 6b & d) we examined the distribution of fluorescein-dextran after injection into the left hemisphere.

To allow a qualitative examination of the relative densities of innervation of the three IC subdivisions (Fig. 7b-f), fluorescent puncta of dextran were captured using the 'analyse particles' function in ImageJ and a 'mask' was made for each particle. As the puncta are too small to be visible at low power, for illustration purposes we expanded each mask digitally by a radius of 15 pixels using Adobe Photoshop. To determine whether dextran labelling in terminals was associated with GABAergic or non-GABAergic (putative glutamatergic) neurons, confocal Z-stacks of varying depths (7-15 µm) (x63 oil, 1.40 NA, 1.03 µs pixel dwell time, X-Y dimensions 1024x1024, Z step 0.26 µm, bit depth 8 with linear LUTs) were taken from the immunolabelled sections. Representative Z-stacks were taken in the ICD (2 stacks per animal), ICC (3 stacks per animal), and ICL (1 stack per animal). Z-stacks were cropped post-hoc to 7 µm thickness. The presence of red dextran was imaged in sections in which GABA had been labelled

with AlexaFluor 488 (green) and green dextran was imaged in sections in which GABA had been labelled with AlexaFluor 568 (red).

Using Imaris™ (Bitplane) the DAPI signal was rendered to a 'surface' and the dextran labelling was rendered into 'spots'. The proximity of the dextran 'spots' to DAPI 'surface' was measured, allowing us to assess whether dextran labelled terminals were in close proximity (≤ 3 µm) to cell somata. Note: we immunolabelled NeuN to visualise more of the cell body and proximal processes of the IC neurons to allow us to examine whether dextran labelled terminals contacted somatic or dendritic sites. However, we noted that many DAPI labelled nuclei in the IC which were in close proximity to dextran labelled terminals and in some cases were also labelled for GABA, and so were presumed to be neurons, do not label for NeuN. Hence we used the DAPI nuclear signal rather than NeuN to define cell somata.

Experimental Design and Statistical Analysis

This study describes largely qualitative data on the distribution of retrograde and anterograde tracers in the brain.

For **retrograde tracing** experiments, eight animals received injections of Retrobeads: red in the right and green in the left IC. For each animal, sections through the whole brain were visually inspected using a widefield microscope. The presence of both red and green beads in both hemispheres was recorded. For quantification we selected six sections (distributed rostrocaudally through the brain) from three animals. All cells containing red Retrobeads were counted in each section in both hemispheres, dividing cortical areas according to the atlas of Paxinos and Watson (1998). Descriptive statistics (mean and SEM) for the raw cell counts and for the percentage in each hemisphere are presented. No statistical comparisons were made.

For **anterograde tracing** experiments, ten animals received injections of fluorescent dextran: five received one injection (right side only) and five received two injections (one right, one left). Red and green dextran were injected into the right and left hemispheres, respectively (Table 1). From these animals, the whole of the IC was sectioned and visually inspected using a widefield microscope and the distribution of dextran recorded. Distribution of the terminal fields in the subdivisions of the IC were studied using one IC section from one animal with an injection in each of the cortical regions of interest. To examine lateralisation, one IC section from one animal with an injection in the motor cortex and one animal with an injection in the auditory cortex were selected. Dextran spots were counted in five Z-stacks of regions of interest (160 μm^2, 7µm thickness (one in IC_D and IC_L, and 3 in IC_C)) in both hemispheres. Descriptive statistics (mean and SEM) of the percentage of dextran spots in each hemisphere are presented. No statistical comparisons were made. To examine the distribution of dextran around GABA labelled elements, one section from individual animals with injections in the prefrontal (n=1), motor (n=1), auditory (n=2), visual (n=2), and somatosensory (n=2) cortices were immuno labelled for GABA. These sections were visually inspected at high power (x40) and photographs representative of the distribution of dextran relative to GABA labelled elements were taken.

RESULTS

Retrograde labelling

Injection sites

We injected red Retrobeads into the right IC and green Retrobeads into the left IC of 8 rats (see Methods). Retrobead injection sites in all animals were inspected using a wide-field microscope. At the injection site very bright beads could be seen. In all but one case Retrobead injections were well placed: one green Retrobead injection was misplaced and the data from this injection was discounted. Correctly placed injections (n=15) were centred in the IC_C and included the lateral part of the IC_D: in some cases there was some spread of Retrobeads into IC_L. All injections were contained entirely within

the boundaries of the IC. Notably, there was no upward spread of Retrobeads into the visual cortex which overlies the IC. From the larger group of injections, the red Retrobead injections in three animals (R4, R5 and R6) were chosen for quantitative analysis. Figure 1 shows the extent of the red Retrobead injection in in the right IC in these animals traced from x20 confocal mosaic images.

Retrograde labelling from the IC is seen in multiple cortical areas in both the ipsi- and contra-lateral hemispheres

As a positive control for our retrograde labelling, we first examined the presence of Retrobeads in the auditory cortex ipsilateral and contralateral to the injection site (henceforth referred to as the ipsilateral and contralateral cortices). As anticipated, Retrobeads injected in the ICC/ICD labelled many neurons in both the ipsilateral and contralateral auditory cortex, predominantly at a depth consistent with layer V (Fig. 2a). Labelling was evident as distinct bright beads which are associated with DAPI stained nuclei suggesting that the beads are located within cell somata. The subcellular distribution of the Retrobeads and the orientation of the labelled cells indicates they are pyramidal neurons (Fig. 2b).

In addition to the labelling seen in the auditory cortex, large numbers of Retrobead-labelled neurons were also seen in many non-auditory cortical areas. Indeed, labelling extended from the visual areas caudally all the way to the prefrontal regions rostrally. Large numbers of neurons containing Retrobeads were found in visual cortex (Fig. 3a), somatosensory cortex (Fig. 3c), motor cortex (Fig. 3d and e) and prefrontal cortex (Fig. 3f, see also Table 2). As in auditory cortex (Fig. 3b), Retrobeads were predominantly in the cell soma however, in comparison to the labelling in auditory cortex (Fig. 3b) in non-auditory cortical areas (Fig. 3a, c-f) the density of Retrobeads in each cell appeared lower.

Visual Cortex

Retrogradely labelled neurons were found in both ipsi- and contralateral visual cortices (Figs. 4a & b, 5a & b; Table 2). They were numerous in both primary visual cortex (monocular and binocular) and secondary visual cortex (lateral area and mediolateral area) (Figs. 4a & b, 5a & b). Caudally, labelled cells were found in a wide band (Figs. 4a, 5a) whereas more rostrally retrogradely labelled cells were concentrated in the deeper part of the cortical thickness (Fig. 4b, 5b). Quantification of the labelled neurons (in two sections from each of 3 animals) revealed a consistently high degree of lateralization. Thus, although retrograde labelling was bilateral, there were far fewer labelled neurons in the contralateral compared to the ipsilateral visual cortices (Figs. 4a, b and h, 5a & b; Table 2).

Auditory cortex

As expected (see Introduction), retrograde labelling was seen in both the ipsi- and contralateral auditory cortices (Figs. 4b & c, 5b & c; Table 2). Many labelled neurons were present in the primary auditory cortex (Au1), and both dorsal (AuD) and ventral (AuV) secondary auditory cortices (Fig. 4b & c, 5b & c). On the ipsilateral side labelled neurons were densely packed in presumed layer V with a few in layer VI, whereas on the contralateral side, the labelled neurons were scattered over a wider band (Figs. 4b & c, 5b & c). As in the visual cortex, we observed many fewer retrogradely labelled neurons in the contralateral compared to the ipsilateral auditory cortex (Fig. 4h; Table 2).

Somatosensory cortex

A second major non-auditory sensory cortical region which contained a substantial number of retrogradely labelled neurons was the somatosensory cortex. As was the case in the auditory and visual cortices, in the somatosensory cortex labelling was present in both ipsi- and contralateral hemispheres (Figs. 4c, d & e, 5c, d & e; Table 2). Primary somatosensory regions (S1) with large numbers of retrogradely labelled cells included the trunk, forelimb, hindlimb, dorsal zone, and jaw areas. Note that although there are relatively few cells in the barrel field of case R5 (shown in Fig. 4c), R4 and R6 did have some labelled neurons in this region (Fig 5c). Secondary somatosensory areas (S2)

also contained large numbers of retrogradely-labelled cells (Figs. 4c & 5c). In more rostral sections the width of the band of labelled cells increases consistent with the increased thickness of the cortical layers (Fig. 4d & e, 5 d & e). Interestingly, while there were more labelled neurons ipsilateral than contralateral to the injected IC, this difference was not as great as that observed in the auditory and visual cortices (Fig. 4h; Table 2).

Motor cortex

Outside the sensory domain, we also found retrograde labelling from the IC in the motor cortex. Here, as in other cortical regions, labelling was evident in both ipsi- and contra-lateral sides. Many labelled neurons were seen in both the primary motor cortex (M1) and secondary motor cortex (M2) (Figs. 4d, e and f; 5d, e and f; Table 2), and labelling extended along the whole rostro-caudal extent of the motor cortices. On both ipsi- and contralateral sides labelled neurons were dispersed more widely through the cortical thickness. It was notable that in motor areas, the lateralization pattern of retrograde labelling resembled that seen in the somatosensory regions in that only marginally fewer labelled neurones were found in the contralateral compared to the ipsilateral side (Fig 4h; Table 2).

Prefrontal cortex

The prefrontal cortex lies at the most rostral end of the cerebral cortex and comprises both the medial prefrontal and orbitofrontal regions. Following Retrobead injections into the IC many labelled neurons were found in the prefrontal cortex of both hemispheres (Figs. 3b, 4d-f, 5d-f; Table 2).

The medial prefrontal cortex, which subserves executive function, is distinct in that its laminae lie dorso-ventrally. Retrograde labelled neurons were concentrated in the cingulate (Cg1 and Cg2) and prelimbic (PrL) cortices, and there were few, if any, labelled neurons in the more ventral infralimbic (IL) and dorsal peduncular (DP) regions. Retrogradely labelled neurons were located in the middle and deep part of the cortex thickness close to the white matter of the forceps minor. The orbitofrontal cortex, which is situated ventral to the forceps minor, integrates sensory and autonomic information.

In orbitofrontal cortex, retrograde labelled neurons were observed in the ventral (VO) and lateral LO) regions with fewer labelled neurons in the medial (MO) orbitofrontal cortex. Retrograde labelled neurons were located more deeply. Considering the prefrontal cortex as a whole (Cg1, Cg2, PrL, IL, DP, VO, MO and LO), the degree of lateralization was low with almost as many retrogradely labelled neurons on the contralateral side (44%) as on the ipsilateral side (56%) (Fig 4h; Table 2).

As is evident from Table 2, the number of labelled neurons counted in different cortical regions varies considerably. Such cell counts cannot, however, be used to infer differences in the degree of connectivity between cortical regions and the IC for two reasons. First, the area within a section occupied by some cortical regions is considerably greater than others (see Table 2), and some regions extend to more than one section (see Fig 4a-f & 5a-f). Second we have only counted representative sections, not the whole cortex. Thus, cell counts are indicative that connections exist between specific cortical regions and the IC, but do not quantify these connections.

Non-cortical regions are retrogradely labelled from IC

Following Retrobead injections into the IC, labelled cells were also observed in brainstem auditory regions known to innervate the IC (including cochlear nucleus, olivary complex, dorsal nucleus of the lateral lemniscus). In addition, we noted Retrobead-labelled cells in many subcortical forebrain regions including olfactory bulb, caudate putamen, hippocampus, thalamus, hypothalamus and amygdala, as well as in mid- and hindbrain regions including superior colliculus and dorsal raphe (Olthof et al., 2019). The innervation of the IC by these regions will be the subject of a second paper.

Although we concentrated our detailed analysis on the red Retrobeads and quantified retrograde labelling in only a subset of the animals, qualitatively the distribution of retrogradely labelled cells was the same for all red and green Retrobead injections.

Anterograde labelling

To verify our findings with retrograde tracing, and to examine both the regional distribution and neuronal targets of cortical inputs to the IC, we injected anterograde tracers (TRITC- (red) and fluorescein- (green) labelled dextran) into cortical regions of interest and examined the presence of dextran labelled terminals in the ipsi- and contralateral IC. For this purpose, we chose a relatively high molecular weight dextran (10,000 m.wt) conjugated to a fluorophore, in order to highlight terminals and avoid the labelling of other neuronal elements.

Cortical sites of anterograde tracer injections

At the injection site, fluorescent labelling of neuronal elements was intense and the location and dispersal of the tracer was readily visualised. All injections were correctly placed within the intended cortical region of interest. Although most animals had two cortical injection sites (one red (right) one green (left)), we selected just one of these sites in each animal. As a result, labelling originating from one prefrontal and one motor cortex injection, and two auditory, two visual, and two somatosensory cortical injections were studied in detail (Fig. 6a-d).

Anterograde labelling confirms non-auditory cortical projections to IC

For each of the cortical regions of interest highlighted by our retrograde findings (visual, auditory, somatosensory, motor, and prefrontal), injection of dextran (Fig 6; Table 1) resulted in dense anterograde labelling in the IC (Fig. 7). In all cases, dextran labelling which was evident as individual small fluorescent puncta or clusters of puncta (presumed neuronal terminals) was present in all subdivisions (Fig 7). Subdivisions were identified using immunolabelling for nNOS (see Methods) which distinguishes the cortical subdivisions (IC_D and IC_L) from the IC_C (Fig 7a). However, the different cortical sites of injection shown in Fig 6 resulted in different densities and patterns of labelling. For example, whereas the injection in the motor cortex resulted in dense labelling ventro-medially in IC_C and IC_D, the injection in the auditory cortex resulted in dense labelling dorsally in the IC_D and IC_L (e.g. Fig. 7c & e). However, as we only made a few tracer injections in each cortical region and these were

not placed systematically, we cannot draw specific conclusions about these patterns of connectivity between cortical regions and the IC.

Our retrograde labelling showed that the largest difference in the lateralisation of cortico-collicular neurons was between the auditory cortex (24% contralateral) and motor cortex (46% contralateral). Hence, for these two regions, we compared anterograde labelling in the IC ipsi and contralateral to the injection (Fig. 8). For both auditory cortex (Fig. 8a) and motor cortex (Fig. 8b) tracer injections, dextran labelled terminals were observed in both ICs. Counts of dextran spots in five Z-stacks (one in IC_D and IC_L, and 3 in IC_C) obtained from one animal on both the ipsi- and contralateral side confirmed the findings from the retrograde studies, there was evidence for highly lateralised connections from auditory cortex (62.4 ± 2.12 % ipsi- vs. 37.6 ± 1.48 contralateral) contrasting with strongly bilateral connections from the motor cortex (51.5 ± 1.47% ipsi- vs. 49.5 ± 1.97 contralateral).

To investigate the organisation of labelled puncta with respect the cellular morphology of the IC, we calculated the distance of the dextran labelled terminals from DAPI labelled nuclei using the Imaris™ (Bitplane) 'spot' and 'surface' functions. This analysis revealed that the majority of dextran labelled terminals were clustered around DAPI labelled cell nuclei, sometimes apparently extending along proximal processes but within 3 μm of the nucleus (Fig. 9 green puncta). Other labelled terminals were further away from cell somata, presumably on other neuronal elements (Fig. 9 magenta puncta). This pattern of labelling was seen irrespective of the cortical site of injection of the tracer or the subdivision of the IC examined.

<u>Both GABAergic and glutamatergic neurones are targeted by cortical inputs</u>

Sections from our anterograde tracing studies immunolabelled for GABA revealed a high density of GABAergic neurons of various sizes and morphologies in the IC. Regardless of the cortical site at which the dextran tracer was injected, many anterogradely labelled terminals were found in close proximity

both to GABA labelled neurons and to DAPI stained nuclei of cells that did not label for GABA. Since it is well established that IC neurons contain only one of two principal neurotransmitters, glutamate or GABA (Merchán et al., 2005), these non-GABAergic cells were presumed to be glutamatergic neurons (Fig. 10di-iii). Two populations of GABAergic neurons were discerned, large (> 15 µm; Fig. 10ai-iii) and small (<15 µm; Fig. 10bi-iii) (Ito et al., 2009), and dextran labelled terminals were found in close proximity to both. In the IC$_L$ in particular, we saw GABA neurons with extensive dendrites, and dextran labelled terminals were frequently found in close proximity to these structures (Fig. 10ciii). Labelled terminals were also found close to the smaller, finer, GABAergic dendrites seen in IC$_D$ and ICc (Fig. 10ci and cii).

DISCUSSION

The main finding of this study is that multiple regions of the cerebral cortex make extensive bilateral connections with all three subdivisions of the IC. In addition to previously well-established cortico-collicular inputs from the auditory cortex, we demonstrate substantial connections from visual, somatosensory, motor, and prefrontal regions. Retrograde tracing shows that connections from the ipsilateral side are the most abundant. However, the ipsi-/contralateral difference is less pronounced for somatosensory, motor and prefrontal cortices, where numbers of labelled neurons are nearly equal, than for the visual and auditory cortices where the difference is approximately threefold. Cortico-collicular neurons are most abundant in the deeper part of the cortical thickness, but in some regions, the motor and prefrontal cortices in particular, they are distributed more widely. Anterograde tracing suggests that these cortico-collicular inputs synapse with both GABAergic and glutamatergic neurons in all three divisions of the IC. A surprising aspect of our results is the extent to which diverse cortical projections target the IC$_C$, the main recipient of *ascending* input from brainstem auditory nuclei and traditionally regarded as a centre of auditory processing (Oliver, 2005; Ito and Malmierca, 2018).

Technical considerations

The combined application of retrograde and anterograde tracing methods provides convincing evidence for the existence of cortico-collicular connections from non-auditory cortical regions. Retrobeads show minimal diffusion (Katz et al., 1984) and our injections which targeted ICC and ICD resulted in minimal spread into ICL. Importantly, no Retrobeads were observed in the overlying visual cortex. Thus, we can be confident that the cortical labelling we observed resulted from retrograde transport from the IC. Although we quantified data using red Retrobeads from three exemplar animals, we saw the same pattern of labelling with both red and green Retrobeads in all eight animals.

There were differences in the density of Retrobead labelling of neurons, both within and between regions. Retrobeads are considered efficient tracers, nevertheless differences in the density of labelling of neighbouring cortical neurons have been reported previously (Schofield et al., 2007). Such differences may relate to the number of terminals, their pattern of distribution in the IC, or even to the level of neuronal activity. Differences in labelling density are unlikely to be explained by the distance from the IC to the soma as both densely and less densely labelled cells were found in all cortical regions.

Auditory and non-auditory cortico-collicular projections

Our tracing showed a dense and highly lateralised projection from the auditory cortex to the three subdivisions of the IC. This is consistent with earlier studies (see Introduction and (Winer, 2005; Schofield, 2010; Bajo and King, 2013) for reviews), and serves as a positive control for our exploration of non-auditory cortico-collicular connections. In addition to connections from the auditory cortex, we demonstrate extensive bilateral cortico-collicular projections from visual, somatosensory, motor, and prefrontal cortices. Although we reveal the full extent of these connections, evidence pointing to the existence of some of these non-auditory cortico-collicular connections can be found in an earlier degeneration study in cat by Cooper and Young (1976). Following large lesions of the visual,

somatosensory or motor cortices, these authors reported degenerating fibres in the ipsilateral IC. Although not quantified, their figures suggest that these connections are sparse and mostly confined to areas equivalent to ICD and ICL. Similar findings were reported by RoBards et al. (1976); (1979) for somatosensory cortex. More recently, Lesicko et al. (2016), using anterograde tracing, demonstrated connections from somatosensory cortex to the IC in mouse, but they only reported on the presence of labelled terminals in the 'neurochemical modules' in ICL (Chernock et al., 2004) that were also recipients of somatosensory inputs from the dorsal column and spinal trigeminal nuclei. In our study, we observed connections distributed widely throughout all IC subdivisions, importantly including ICC.

In the case of visual cortex, we observed extensive cortico-collicular connections from both V1 and V2 to the IC. Several functional studies in IC have reported visual modulation of neuronal responses to sounds, and even neuronal responses to visual stimuli alone (Syka and Radil-Weiss, 1973; Tawil et al., 1983; Mascetti and Strozzi, 1988; Porter et al., 2007; Bulkin and Groh, 2012). In the cortices of the IC these interactions may be explained by direct, but sparse, retinal input (Itaya and Van Hoesen, 1982; Yamauchi and Yamadori, 1982). However, responses to visual stimuli or saccades have also been reported, in ICC, albeit with lower prevalence than in the IC cortices (Porter et al., 2007; Bulkin and Groh, 2012). The longer latency responses observed by Porter et al. (2007) are consistent with effects mediated by indirect pathways via the superior colliculus (Adams, 1980; Coleman and Clerici, 1987), or from the visual cortical input we describe here.

The existence of connections from the visual cortex to the IC may explain recent functional studies in which the BOLD response recorded in the IC using fMRI was shown to be influenced by ablation or optogenetic modulation of the visual cortex (Gao et al., 2015; Leong et al., 2018). Interestingly, the results of these studies implied that input from visual cortex enhanced response gain, whereas input from the auditory cortex reduced gain. Although cortical output projections are considered exclusively excitatory, our finding that projections from cortical regions terminate on both GABAergic and

presumed glutamatergic neurons shows that di-synaptic circuits in the IC can readily transform cortically mediated excitation to inhibition.

We also demonstrate feedback connections from motor cortex to the IC. These may be important for two reasons. First, they could be a source of feedback about self-generated sounds – such as vocalisations and sounds resulting from an animal's interaction with its environment (Schneider and Mooney, 2018; Schneider et al., 2018). Interestingly, neurons in the IC respond prior to vocalisation and the IC projects to the neighbouring periaqueductal gray (Moore and Goldberg, 1966; Carey and Webster, 1971), a region involved in the control of vocalisation (Jürgens, 1994; Pieper and Jürgens, 2003). Motor and somatosensory cortical feedback to the IC could also provide predictive information that enables self-generated sounds to be discounted in the parsing of simultaneous sound sources. That neurons throughout the motor cortex project to the IC suggests that body movements may contribute to this process, perhaps via efference copy, and that such feedback is not limited to the control of vocalisation (Schneider and Mooney, 2018). A second reason why motor inputs to the IC are significant is that the IC is one of a network of brain centres involved in escape and other fear responses to aversive sounds. Blockade of inhibition and modulation of NMDA receptors in the IC triggers such behaviours (Brandão et al., 1988; Cardoso et al., 1994; Nobre et al., 2004) and auditory responses in IC are enhanced by unconditioned and conditioned fear evoking stimuli (Brandao et al., 2001). Furthermore, connections from the auditory cortex to the IC have been shown to be important in mediating sound-evoked defence responses (Xiong et al., 2015).

We know of no existing evidence that the prefrontal cortex influences responses in the IC. However, neurons in the orbitofrontal regions respond to sound and, via descending connections, influence sound processing in auditory cortex (Fritz et al., 2010; Schneider et al., 2014; Schneider et al., 2018; Winkowski et al., 2018). These prefrontal cortical regions have a central role in executive function and exert task-dependent influences on sensory processing (Öngür and Price, 2000). Our results demonstrate direct projections from the medial and orbital prefrontal cortex to the IC and suggest

516 that higher-level cognitive functions, including goal directed behaviour, directly affect auditory
517 processing in the midbrain.
518
519 Interestingly, whereas neurons projecting to the IC from the visual and auditory cortices displayed a
520 marked ipsilateral dominance, those in the somatosensory, motor, and prefrontal cortices were less
521 lateralised. This might reflect the fact that movement elicited sounds and cognitive mechanisms are
522 not as strongly lateralised as sources of auditory and visual signals.
523
524 Extensive descending input to the IC from the cerebral cortex indicates that the IC is more than an
525 integrator of ascending auditory signals. These descending inputs are diverse and include other non-
526 auditory sensory areas as well as non-sensory regions. This diversity of cortical projections suggests
527 that different sensory, motor and cognitive cortical influences operate at an early stage of processing
528 to influence an animal's perceptual and behavioural responses to sound. We can only speculate about
529 the precise function of this multisystem feedback and how it might mediate the signals required to
530 identify sounds in sound-cluttered environments. The mechanisms involved could subserve predictive
531 coding, using priors derived from stimulus history, efference copy to discount self-generated sounds,
532 and the transforms of coordinate frames of reference that enable the senses to be integrated into a
533 coherent representation.
534
535 Our data show that multisystem networks sub-serving sensory, motor and executive function extends
536 to subcortical structures. As discussed in the Introduction, there is mounting evidence for the top-
537 down modulation of sensory signals, as well as cortico-cortical connections mediating interactions
538 between sensory modalities. Taken together, these data demand a revision of current models of
539 sensory perception.
540
541 **AUTHOR CONTRIBUTIONS**

BMJO, AR and SEG all contributed to the design of the experiments and the injection of tracers. BMJO and SEG processed and BMJO imaged the resulting tissue. BMJO, AR and SEG wrote and edited the manuscript.

REFERENCES

Adams JC (1980) Crossed and descending projections to the inferior colliculus. Neurosci Lett 19:1-5.

Aitkin LM, Kenyon CE, Philpott P (1981) The representation of the auditory and somatosensory systems in the external nucleus of the cat inferior colliculus. J Comp Neurol 196:25-40.

Aitkin LM, Dickhaus H, Schult W, Zimmermann M (1978) External nucleus of inferior colliculus: Auditory and spinal somatosensory afferents and their interactions. J Neurophysiol 41:837-847.

Andersen RA, Snyder RL, Merzenich MM (1980) The topographic organization of corticocollicular projections from physiologically identified loci in the ai, aii, and anterior auditory cortical fields of the cat. J Comp Neurol 191:479-494.

Bajo VM, Moore DR (2005) Descending projections from the auditory cortex to the inferior colliculus in the gerbil, *Meriones unguiculatus*. J Comp Neurol 486:101-116.

Bajo VM, King AJ (2013) Cortical modulation of auditory processing in the midbrain. Frontiers in Neural Circuits 6.

Bajo VM, Nodal FR, Bizley JK, Moore DR, King AJ (2007) The ferret auditory cortex: Descending projections to the inferior colliculus. Cereb Cortex 17:475-491.

Bastos AM, Usrey WM, Adams RA, Mangun GR, Fries P, Friston KJ (2012) Canonical microcircuits for predictive coding. Neuron 76:695-711.

Beyerl BD (1978) Afferent projections to the central nucleus of the inferior colliculus in the rat. Brain Res 145:209-223.

Brandao ML, Coimbra NC, Osaki MY (2001) Changes in the auditory-evoked potentials induced by fear-evoking stimulations. Physiol Behav 72:365-372.

Brandão ML, Tomaz C, Leão Borges PC, Coimbra NC, Bagri A (1988) Defense reaction induced by microinjections of bicuculline into the inferior colliculus. Physiol Behav 44:361-365.

Budinger E, Heil P, Scheich H (2000) Functional organization of auditory cortex in the mongolian gerbil (Meriones unguiculatus). IV. Connections with anatomically characterized subcortical structures. Eur J Neurosci 12:2452-2474.

Bulkin DA, Groh JM (2012) Distribution of visual and saccade related information in the monkey inferior colliculus. Front Neural Circuits 6:61.

Cardoso SH, Coimbra NC, Brandao ML (1994) Defensive reactions evoked by activation of nmda receptors in distinct sites of the inferior colliculus. Behav Brain Res 63:17-24.

Carey CL, Webster DB (1971) Ascending and descending projections of the inferior colliculus in the kangaroo rat *(Dipodomys merriami)*. Brain Behav Evol 4:401-412.

Chernock ML, Larue DT, Winer JA (2004) A periodic network of neurochemical modules in the inferior colliculus. Hear Res 188:12-20.

Coleman JR, Clerici WJ (1987) Sources of projections to subdivisions of the inferior colliculus in the rat. J Comp Neurol 262:215-226.

Coomes DL, Schofield RM, Schofield BR (2005) Unilateral and bilateral projections from cortical cells to the inferior colliculus in guinea pigs. Brain Res 1042:62-72.

Cooper MH, Young PA (1976) Cortical projections to the inferior colliculus of the cat. Exp Neurol 51:488-502.

Diamond IT, Jones EG, Powell TPS (1969) The projection of the auditory cortex upon the diencephalon and brain stem in the cat. Brain Res 15:305-340.

Feliciano M, Potashner SJ (1995) Evidence for a glutamatergic pathway from the guinea pig auditory cortex to the inferior colliculus. J Neurochem 65:1348-1357.

Friston K (2005) A theory of cortical responses. Philosophical Transactions of the Royal Society B: Biological Sciences 360:815-836.

Fritz JB, David SV, Radtke-Schuller S, Yin P, Shamma SA (2010) Adaptive, behaviorally gated, persistent encoding of task-relevant auditory information in ferret frontal cortex. Nat Neurosci 13:1011.

Gao PP, Zhang JW, Fan S-J, Sanes DH, Wu EX (2015) Auditory midbrain processing is differentially modulated by auditory and visual cortices: An auditory fMRI study. Neuroimage 123:22-32.

596 Itaya SK, Van Hoesen GW (1982) Retinal innervation of the inferior colliculus in rat and monkey. Brain
597 Res 233:45-52.
598 Ito T, Malmierca MS (2018) Neurons, connections and microcircuits of the inferior colliculus. In: The
599 mammalian auditory pathways: Synaptic organisation and microcircuits (Oliver DL, Cant NB,
600 Fay RR, Popper AN, eds), pp 127 - 168: Springer.
601 Ito T, Bishop DC, Oliver DL (2009) Two classes of gabaergic neurons in the inferior colliculus. J Neurosci
602 29:13860-13869.
603 Jain R, Shore S (2006) External inferior colliculus integrates trigeminal and acoustic information: Unit
604 responses to trigeminal nucleus and acoustic stimulation in the guinea pig. Neurosci Lett
605 395:71-75.
606 Jürgens U (1994) The role of the periaqueductal grey in vocal behaviour. Behav Brain Res 62:107-117.
607 Katz LC, Burkhalter A, Dreyer WJ (1984) Fluorescent latex microspheres as a retrograde neuronal
608 marker for in vivo and in vitro studies of visual cortex. Nature 310:498-500.
609 Kayser C, Logothetis NK (2007) Do early sensory cortices integrate cross-modal information? Brain
610 Struct Funct 212:121-132.
611 Leong ATL, Dong CM, Gao PP, Chan RW, To A, Sanes DH, Wu EX (2018) Optogenetic auditory fMRI
612 reveals the effects of visual cortical inputs on auditory midbrain response. Scientific Reports
613 8:8736.
614 Lesicko AM, Hristova TS, Maigler KC, Llano DA (2016) Connectional modularity of top-down and
615 bottom-up multimodal inputs to the lateral cortex of the mouse inferior colliculus. J Neurosci
616 36:11037-11050.
617 Mascetti GG, Strozzi L (1988) Visual cells in the inferior colliculus of the cat. Brain Res 442:387-390.
618 Merchán M, Aguilar LA, Lopez-Poveda EA, Malmierca MS (2005) The inferior colliculus of the rat:
619 Quantitative immunocytochemical study of gaba and glycine. Neuroscience 136:907-925.
620 Moore RY, Goldberg JM (1966) Projections of the inferior colliculus in the monkey. Exp Neurol 14:429-
621 438.
622 Nobre MJ, Lopes MG, Brandao ML (2004) Defense reaction mediated by nmda mechanisms in the
623 inferior colliculus is modulated by gabaergic nigro-collicular pathways. Brain Res 999:124-131.
624 Oliver DL (2005) Neuronal organisation of the inferior colliculus. In: The inferior colliculus (Winer JA,
625 Schreiner CE, eds), pp 69-114. New York: Springer.
626 Olthof BM, Gartside SE, Rees A (2019) Non-auditory projections to the inferior colliculus. In: Assoc.
627 Res. Otolaryngol. Abs.:, p 351.
628 Öngür D, Price JL (2000) The organization of networks within the orbital and medial prefrontal cortex
629 of rats, monkeys and humans. Cereb Cortex 10:206-219.
630 Paxinos G, Watson C (1998) The rat brain in stereotaxic coordinates, Fourth Edition. San Diego:
631 Academic Press.
632 Pieper F, Jürgens U (2003) Neuronal activity in the inferior colliculus and bordering structures during
633 vocalization in the squirrel monkey. Brain Res 979:153-164.
634 Porter KK, Metzger RR, Groh JM (2007) Visual- and saccade-related signals in the primate inferior
635 colliculus. Proc Natl Acad Sci U S A 104:17855-17860.
636 Rao RPN, Ballard DH (1999) Predictive coding in the visual cortex: A functional interpretation of some
637 extra-classical receptive-field effects. Nat Neurosci 2:79.
638 Robards MJ (1979) Somatic neurons in the brainstem and neocortex projecting to the external nucleus
639 of the inferior colliculus: An anatomical study in the opossum. J Comp Neurol 184:547-565.
640 RoBards MJ, Watkins DW, 3rd, Masterton RB (1976) An anatomical study of some somesthetic
641 afferents to the intercollicular terminal zone of the midbrain of the opossum. J Comp Neurol
642 170:499-524.
643 Saldana E, Feliciano M, Mugnaini E (1996) Distribution of descending projections from primary
644 auditory neocortex to inferior colliculus mimics the topography of intracollicular projections.
645 J Comp Neurol 371:15-40.

646 Schindelin J, Arganda-Carreras I, Frise E, Kaynig V, Longair M, Pietzsch T, Preibisch S, Rueden C, Saalfeld
647 S, Schmid B, Tinevez J-Y, White DJ, Hartenstein V, Eliceiri K, Tomancak P, Cardona A (2012) Fiji:
648 An open-source platform for biological-image analysis. Nature Methods 9:676.
649 Schneider DM, Mooney R (2018) How movement modulates hearing. Annu Rev Neurosci 41:553-572.
650 Schneider DM, Nelson A, Mooney R (2014) A synaptic and circuit basis for corollary discharge in the
651 auditory cortex. Nature 513:189.
652 Schneider DM, Sundararajan J, Mooney R (2018) A cortical filter that learns to suppress the acoustic
653 consequences of movement. Nature 561:391-395.
654 Schofield BR (2010) Structural organization of the descending auditory pathway. In: The auditory brain
655 (Rees A, Palmer AR, eds), pp 43-64. Oxford: Oxford University Press.
656 Schofield BR, Schofield RM, Sorensen KA, Motts SD (2007) On the use of retrograde tracers for
657 identification of axon collaterals with multiple fluorescent retrograde tracers. Neuroscience
658 146:773-783.
659 Syka J, Radil-Weiss T (1973) Acoustical responses of inferior colliculus neurons in rats influenced by
660 sciatic nerve stimulation and light flashes. Int J Neurosci 5:201-206.
661 Tawil RN, Saadé NE, Bitar M, Jabbur SJ (1983) Polysensory interactions on single neurons of cat inferior
662 colliculus. Brain Res 269:149-152.
663 Watson RE, Wiegand SJ, Clough RW, Hoffman GE (1986) Use of cryoprotectant to maintain long-term
664 peptide immunoreactivity and tissue morphology. Peptides 7:155-159.
665 Winer JA (2005) Descending input to the midbrain. In: The inferior colliculus (Winer JA, Schreiner CE,
666 eds), pp 231-247. New York: Springer.
667 Winer JA, Larue DT, Diehl JJ, Hefti BJ (1998) Auditory cortical projections to the cat inferior colliculus.
668 J Comp Neurol 400:147-174.
669 Winkowski DE, Nagode DA, Donaldson KJ, Yin P, Shamma SA, Fritz JB, Kanold PO (2018) Orbitofrontal
670 cortex neurons respond to sound and activate primary auditory cortex neurons. Cereb Cortex
671 28:868-879.
672 Xiong XR, Liang F, Zingg B, Ji X-y, Ibrahim LA, Tao HW, Zhang LI (2015) Auditory cortex controls sound-
673 driven innate defense behaviour through corticofugal projections to inferior colliculus. Nature
674 Communications 6:7224.
675 Yamauchi K, Yamadori T (1982) Retinal projection to the inferior colliculus in the rat. Cells Tissues
676 Organs 114:355-360.

677 **Table 1. Anterograde injection sites**

RAT IDENTIFIER	RIGHT	LEFT
ANTEROGRADE 1	Auditory *	-
ANTEROGRADE 2	Auditory *	-
ANTEROGRADE 3	Auditory	-
ANTEROGRADE 4	Auditory	-
ANTEROGRADE 5	Prefrontal *	Visual
ANTEROGRADE 6	Motor *	-
ANTEROGRADE 7	Visual *	Prefrontal
ANTEROGRADE 8	Prefrontal	Visual *
ANTEROGRADE 9	Somatosensory *	Prefrontal
ANTEROGRADE 10	Visual	Somatosensory *

678

679 TRITC-labelled dextran (red) was always injected into the right hemisphere
680 and fluorescein-labelled dextran (green) was injected into the left
681 hemisphere. Asterisk indicates the animals/injections which were used in
682 the immunohistochemistry studies.

683 **Table 2. Retrogradely labelled cells in cortical regions**

Area (mm^2)		Ipsilateral R 4	Ipsilateral R 5	Ipsilateral R 6	Ipsilateral Mean	Contralateral R 4	Contralateral R 5	Contralateral R 6	Contralateral Mean
PFC	count	439	595	504	513	362	510	415	429
(10.57)	%	*54.9*	*54.7*	*56.2*	*55.3*	*45.1*	*45.3*	*43.8*	*44.7*
M2	count	315	430	262	336	225	294	190	236
(6.31)	%	*57.7*	*60.5*	*59.1*	*59.1*	*42.3*	*39.5*	*40.9*	*40.9*
M1	count	491	565	638	565	401	480	549	477
(11.91)	%	*56.6*	*56.4*	*55.0*	*56.0*	*43.4*	*43.6*	*45.0*	*44.0*
S2	count	73	104	120	99	56	80	100	79
(0.98)	%	*62.2*	*58.2*	*57.2*	*59.2*	*37.8*	*41.8*	*42.8*	*40.8*
S1	count	518	493	430	480	403	355	345	368
(13.60)	%	*57.3*	*60.2*	*57.4*	*58.3*	*42.7*	*39.8*	*42.6*	*41.7*
AuV	count	145	153	59	119	46	51	20	39
(1.41)	%	*75.7*	*75.1*	*75.2*	*75.3*	*24.3*	*24.9*	*24.8*	*24.7*
AuD	count	208	169	57	145	47	60	20	42
(1.70)	%	*81.5*	*74.4*	*74.0*	*76.6*	*18.5*	*25.6*	*26.0*	*23.4*
Au1	count	170	171	124	155	52	55	40	49
(2.45)	%	*76.8*	*75.9*	*75.6*	*76.1*	*23.2*	*24.1*	*24.4*	*23.9*
V2	count	164	103	64	110	83	55	24	54
(9.15)	%	*68.3*	*69.5*	*73.7*	*70.5*	*31.7*	*30.5*	*26.3*	*29.5*
V1	count	31	42	68	47	7	19	22	16
(8.34)	%	*81.6*	*69.4*	*75.9*	*75.6*	*18.4*	*30.6*	*24.1*	*24.4*

684

685 Numbers of Retrobead-labelled cells in each cortical region in each of three representative animals
686 (R4, R5 and R6). Percentages refer to the total number of labelled cells in ipsi- and contralateral
687 hemispheres for each area for each individual animal. Note: cells were counted in the representative
688 sections shown in Figures 4 and 5 in each animal. Note, however, that regions differ in size and some
689 appear in more than one section, thus the total area of each cortical region counted (shown in
690 parentheses) varies between regions. Comparisons of cell counts cannot be used to infer the degree
691 of connectivity different cortical areas have with the IC.

692

693 **Figure 1: Sites of Retrobead injection in the right IC.**

694 For the three animals used for quantitative analysis (**a,** R4, **b,** R5, and **c,** R6), mosaic images were taken and the outline of each injection site
695 was traced in Adobe Illustrator™ and superimposed on corresponding atlas outlines redrawn from Paxinos and Watson (1998). Figures show
696 the rostro-caudal midpoint of the injection.
697
698 **Figure 2: Neurons in the ipsilateral auditory cortex retrogradely labelled from the IC.**

699 Following injection of red Retrobeads into the right ICc/ICd, Retrobeads are found in neurons in the right auditory cortex. Nuclei are labelled
700 with DAPI (blue). **a,** Retrogradely labelled cells are concentrated in a narrow band corresponding to layer V of auditory cortex. **b,** The
701 distribution of beads in the somata highlights the pyramidal cell morphology of the retrogradely labelled neurons.
702
703 **Figure 3: Multiple cortical regions are retrogradely labelled from the IC.**

704 High power maximum intensity projections from confocal Z-stacks showing red Retrobeads in neurons in cortical regions ipsilateral to the
705 injection site. **a.** visual cortex (VC), **b.** auditory cortex (AC), **c.** primary somatosensory cortex (S1), **d.** secondary motor cortex (M2), **e**. primary
706 motor cortex (M1) and **f.** prefrontal cortex (PFC). Nuclei are stained with DAPI (blue).
707
708 **Figure 4: Retrograde cortical labelling demonstrates bilateral inputs from multiple cortical regions to IC.**

709 **a-f,** Confocal mosaic images of coronal cortical sections at multiple locations (shown as distance from bregma) along the rostro-caudal axis
710 (**g**) following the injection of red Retrobeads in the right ICc/ICd in one animal, R5. Red markers indicate cells containing Retrobeads. Cortical
711 divisions are redrawn from the atlas of Paxinos and Watson (1998) and region names are abbreviated on the sections. **h,** Proportions of
712 retrogradely labelled cells in the cortex ipsi- and contralateral to the injected IC as percentage of total labelled neurons in each cortical
713 region. Bars show mean + SEM (n=3 animals) derived from counts made in 2 or 3 sections per animal.
714
715 **Figure 5 retrograde cortical labelling demonstrating inputs from multiple cortical regions to IC in two further representative cases.**

716 **a-f,** Confocal mosaic images of coronal cortical sections at multiple locations (shown by distance from bregma) along the rostro-caudal axis
717 (see Fig 4**g**) following the injection of red Retrobeads in the right ICc/ICd in R4 (left column) and R6 (right column). Red markers indicate cells
718 containing Retrobeads. Cortical regions as marked in Fig 4a-f. These cases with case R5 (Fig. 4a-f) provide the data for the histogram in Fig
719 4h.
720
721 **Figure 6: Sites of anterograde tracer injection in the cortices.**

722 TRITC (red) labelled dextran anterograde tracer was injected in the right hemisphere and fluorescein (green) labelled dextran in the left
723 hemisphere. For the injection sites selected for analysis, mosaic images were taken and the outline of each injection site was traced in Adobe
724 Illustrator™ and superimposed on corresponding atlas outlines redrawn from Paxinos and Watson (1998). Figures show the rostro-caudal
725 midpoint of the injection. Note: each area traced is from a different animal. Injection sites in **a,** prefrontal cortex (Cg1 and PrL, magenta) and
726 motor cortex (M2, red), **b,** somatosensory cortex (S1, red and green), **c,** auditory cortex (Au1, AuD, AuV, PtA, red and magenta), and **d,** visual
727 cortex (V1, green and V1 and V2, red).
728
729 **Figure 7: Distribution of dextran labelled terminals in subdivisions of the IC following anterograde tracer injection into cortical regions.**

730 **a**, Coronal section of IC immunolabelled for nNOS to identify the subdivisions of the IC. IC cortical subdivisions contain neurons whose
731 cytoplasm labels for nNOS. Anterograde labelling from the prefrontal cortex for this section is shown in (b). Similar nNOS Immunolabelling
732 (not shown) was used to define the subdivisions in the remaining cases (c-f). **b-f**, coronal sections of the IC showing the distribution of
733 dextran labelled terminals in the IC following injection of dextran into the cortical region shown above the section. Experimental numbers
734 correspond to Table 1. Terminals were masked and expanded to allow them to be seen at low power (see Methods). Note sections b and f
735 are left ICs but have been reflected in the vertical plane for consistency. The asterisk in (d) shows the site of a fiducial mark where there is
736 no tissue.
737

738 **Figure 8: Anterograde tracing reveals terminals originating from multiple cortical regions target neurons in all IC subdivisions.**
739 Anterograde dextran labelling and were converted into 'spots' and DAPI stained nuclei were converted to 'surfaces' (blue) using Imaris™
740 and the proximity of spots to surfaces was determined. Spots closer than 3µm are colored green and those further away are colored
741 magenta. Distribution of anterograde labelled terminals in ICD, ICC, and ICL (columns left to right) following injections of tracer into visual,
742 auditory, somatosensory, motor and prefrontal cortices (rows top to bottom).
743
744 **Figure 9: Anterograde labelling is present in the ICs both ipsi- and contralateral to the cortical injection.**
745 Anterograde dextran labelling (yellow) in the three subdivisions of the IC (ICD, ICC, and ICL). Dextran injected in **a,** auditory cortex (AC, see
746 Fig 4c). **b,** motor cortex (MC, see Fig4a). Cell nuclei are stained with DAPI (blue).
747
748 **Figure 10: Terminals originating from multiple cortical regions associate with both GABAergic and glutamatergic neurons in the IC.**
749 Confocal Z-stack images showing dextran labelled terminals (yellow) and DAPI stained nuclei (blue). Terminals originating from cortical
750 regions are evident in close proximity to **a,** large GABAergic neurons (red, closed arrows), **b,** smaller GABAergic cells (red, open arrows), and
751 **c,** GABAergic dendrites (red, closed arrowheads). **d,** terminals of cortical origin are also found in close proximity to neurons which do not
752 label for GABA -presumed glutamatergic neurons (open arrowheads). Example confocal images from ICD, ICC, and ICL (columns left to right)
753 showing dextran labelling following injection into visual, somatosensory, motor, or prefrontal cortices (see individual panel labels).

Figure 1

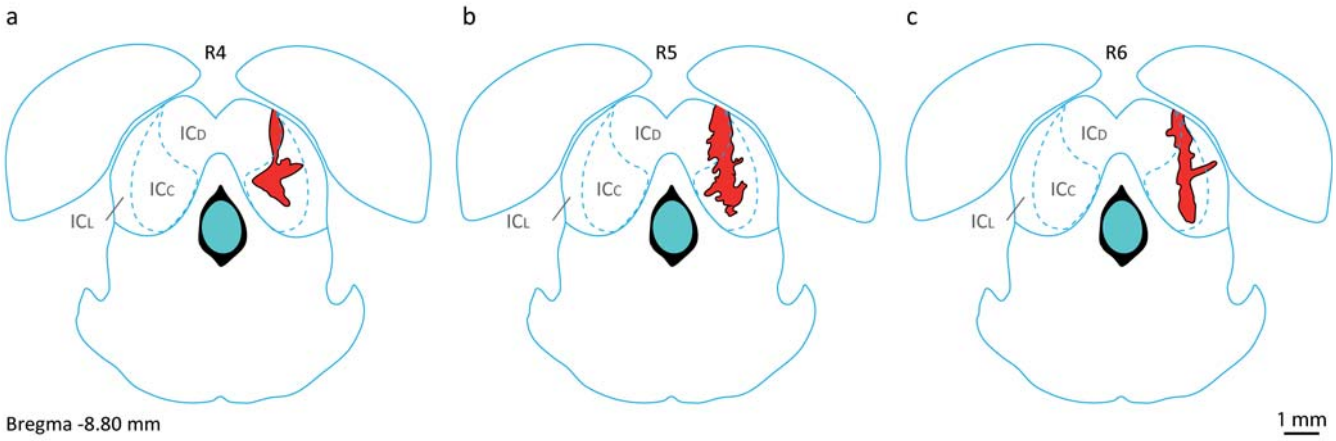
a
R4
ICD
ICC
ICL
b
R5
ICD
ICC
ICL
c
R6
ICD
ICC
ICL
Bregma -8.80 mm
1 mm

Figure 2

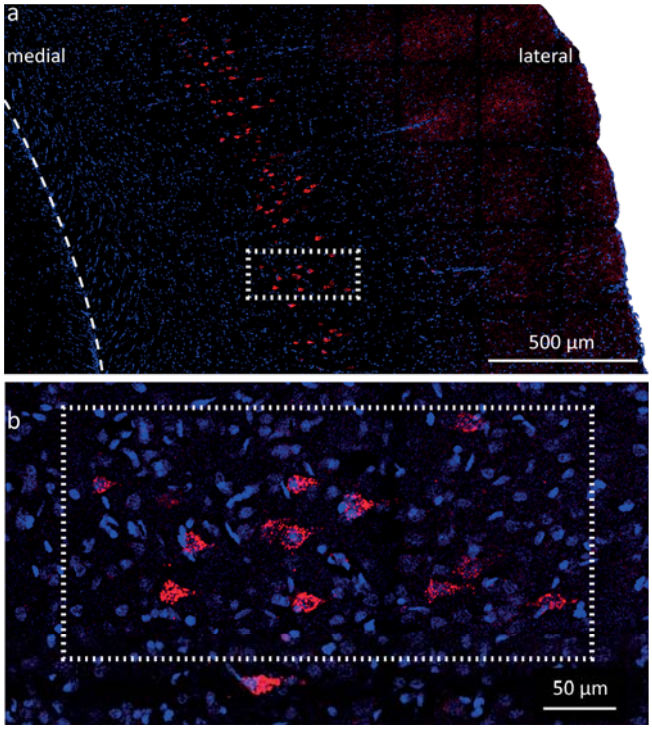

Figure 3

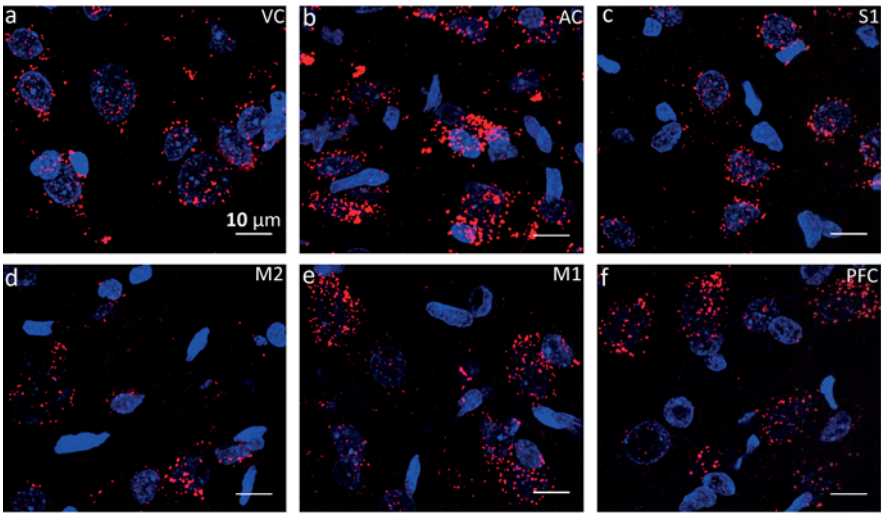

Figure 4

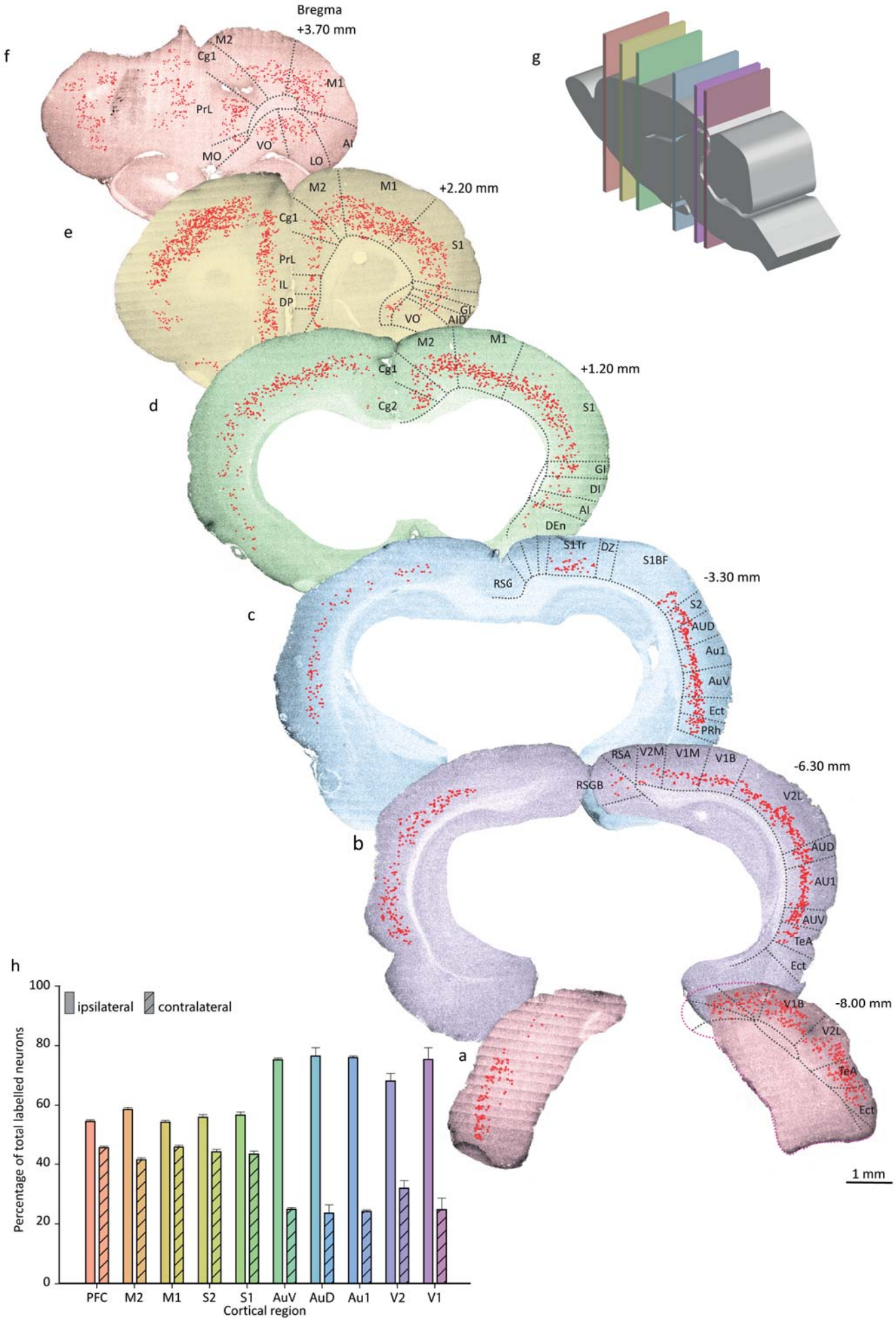
Bregma
+3.70 mm
f
M2
Cg1
M1
PrL
VO
AI
MO
LO
g
+2.20 mm
e
M2
M1
Cg1
S1
PrL
IL
DP
GI
VO
AID
+1.20 mm
d
M2
M1
Cg1
Cg2
S1
GI
DI
AI
DEn
-3.30 mm
c
S1Tr
DZ
S1BF
RSG
S2
AUD
Au1
AuV
Ect
PRh
-6.30 mm
b
RSA
V2M
V1M
V1B
RSGB
V2L
AUD
AU1
AUV
TeA
Ect
-8.00 mm
a
V1B
V2L
TeA
Ect
1 mm
h
ipsilateral
contralateral
Percentage of total labelled neurons
100
80
60
40
20
0
PFC
M2
M1
S2
S1
AuV
AuD
Au1
V2
V1
Cortical region

Figure 5

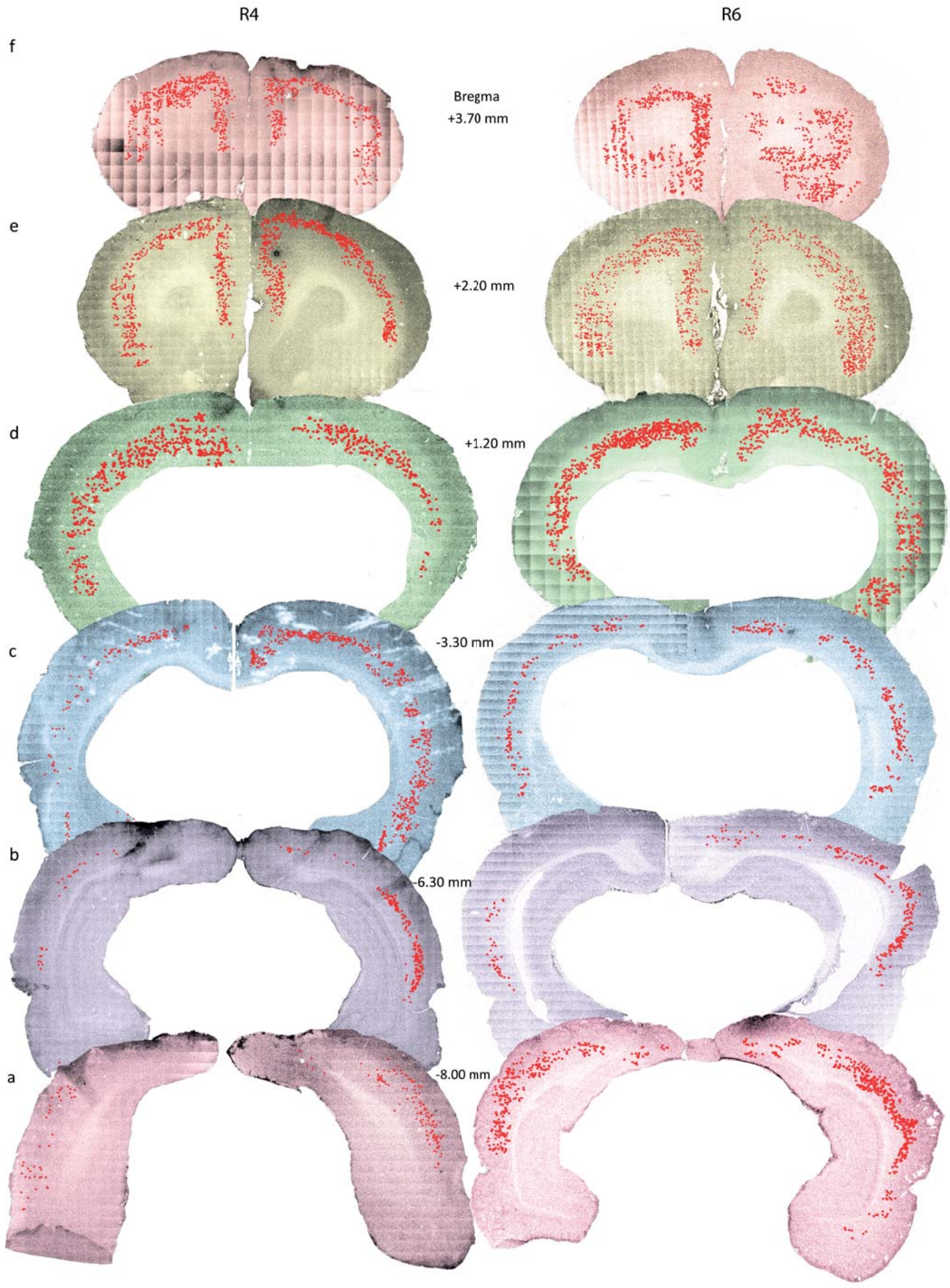

Figure 6

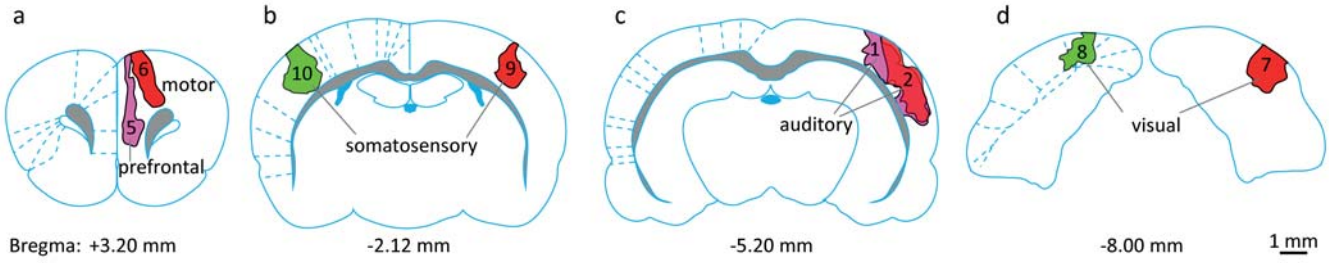
a
6
motor
5
prefrontal
Bregma: +3.20 mm
b
10
9
somatosensory
-2.12 mm
c
1
2
auditory
-5.20 mm
d
8
7
visual
-8.00 mm
1 mm

Figure 7

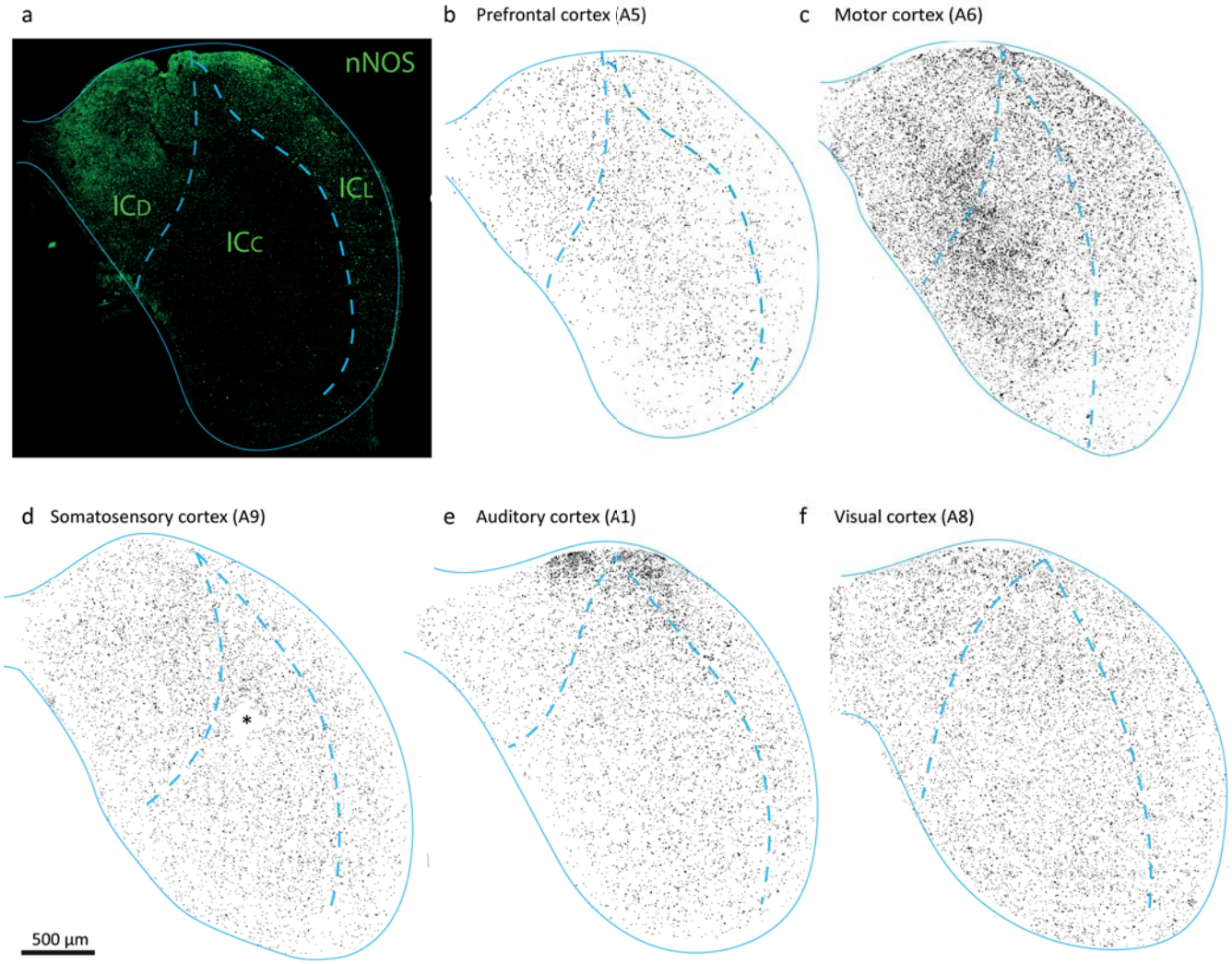
a
nNOS
ICD
ICC
ICL
b Prefrontal cortex (A5)
c Motor cortex (A6)
d Somatosensory cortex (A9)
e Auditory cortex (A1)
f Visual cortex (A8)
500 µm

Figure 8

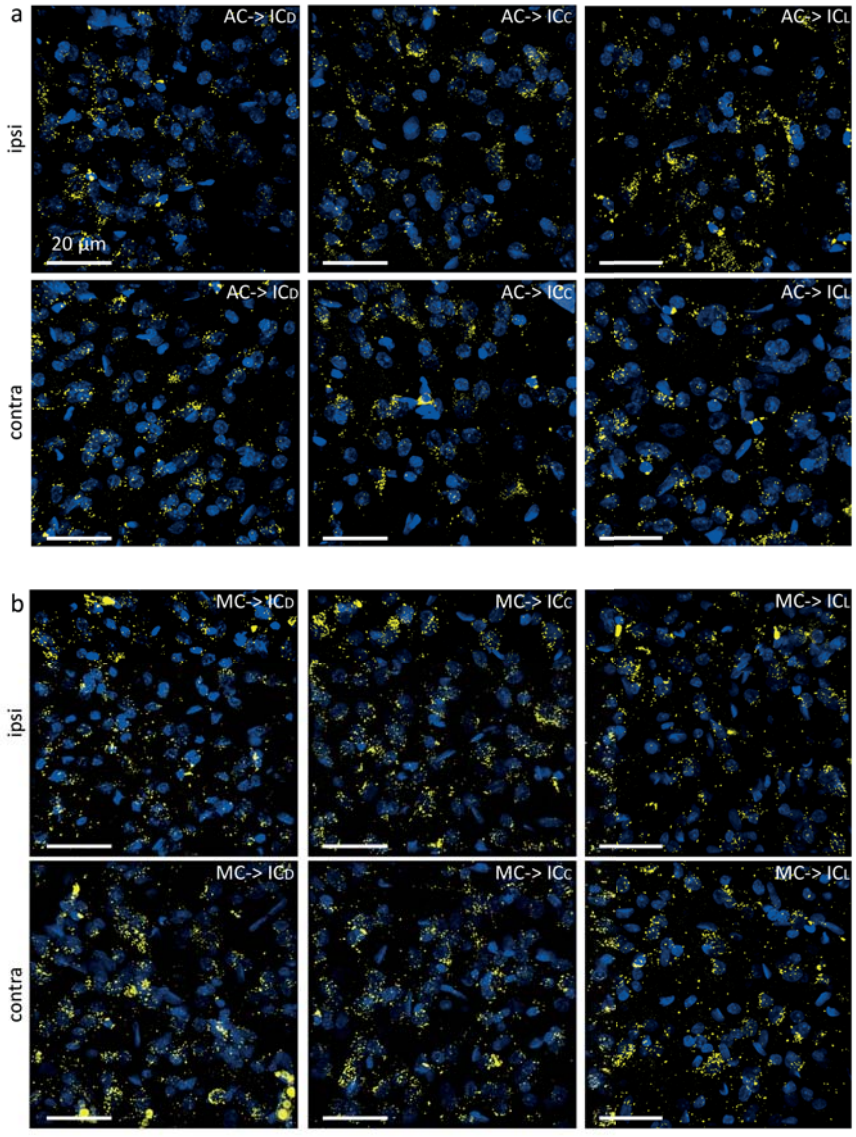

Figure 9

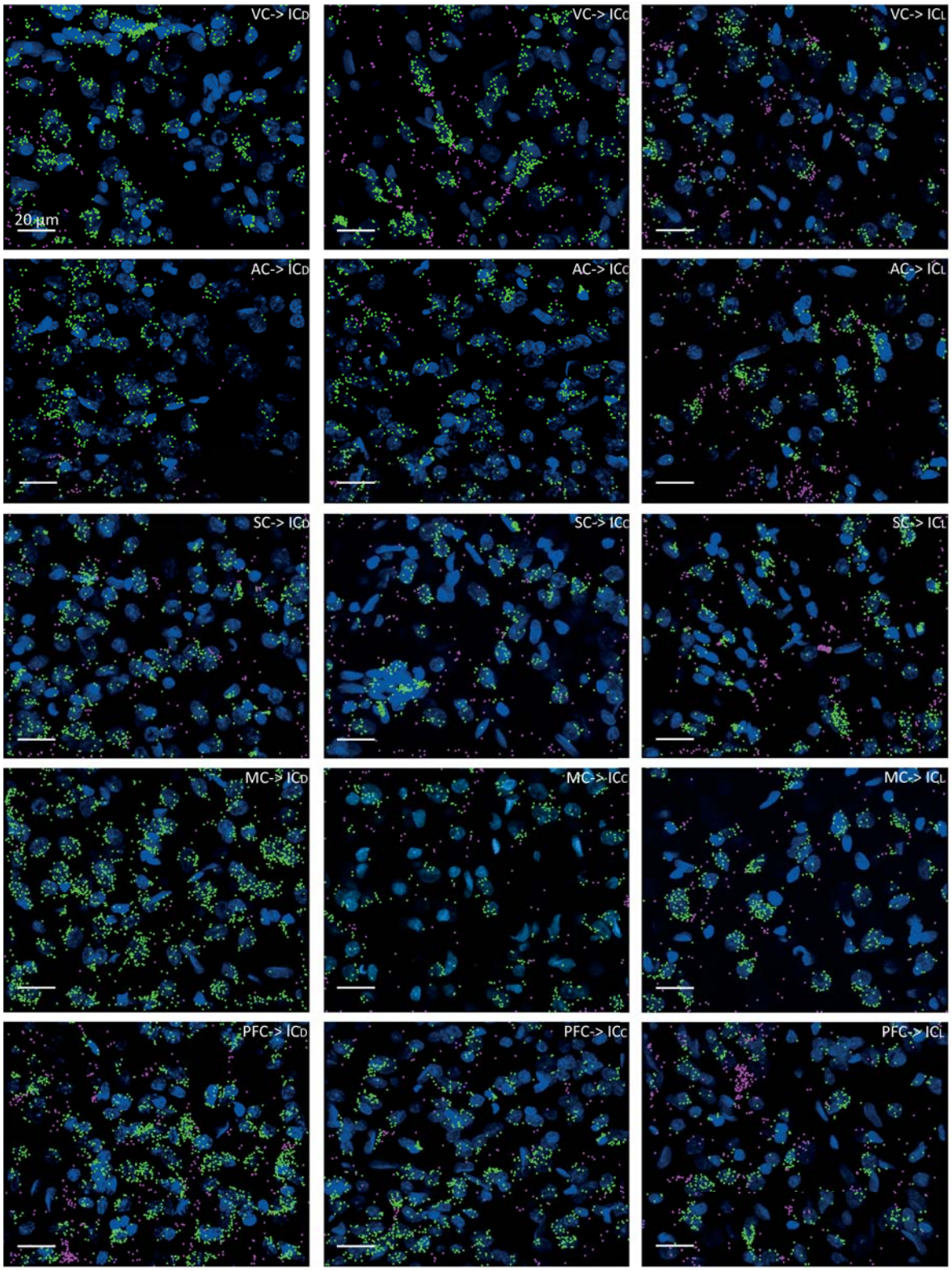
VC-> ICD
VC-> ICC
VC-> ICL
20 µm
AC-> ICD
AC-> ICC
AC-> ICL
SC-> ICD
SC-> ICC
SC-> ICL
MC-> ICD
MC-> ICC
MC-> ICL
PFC-> ICD
PFC-> ICC
PFC-> ICL

Figure 10

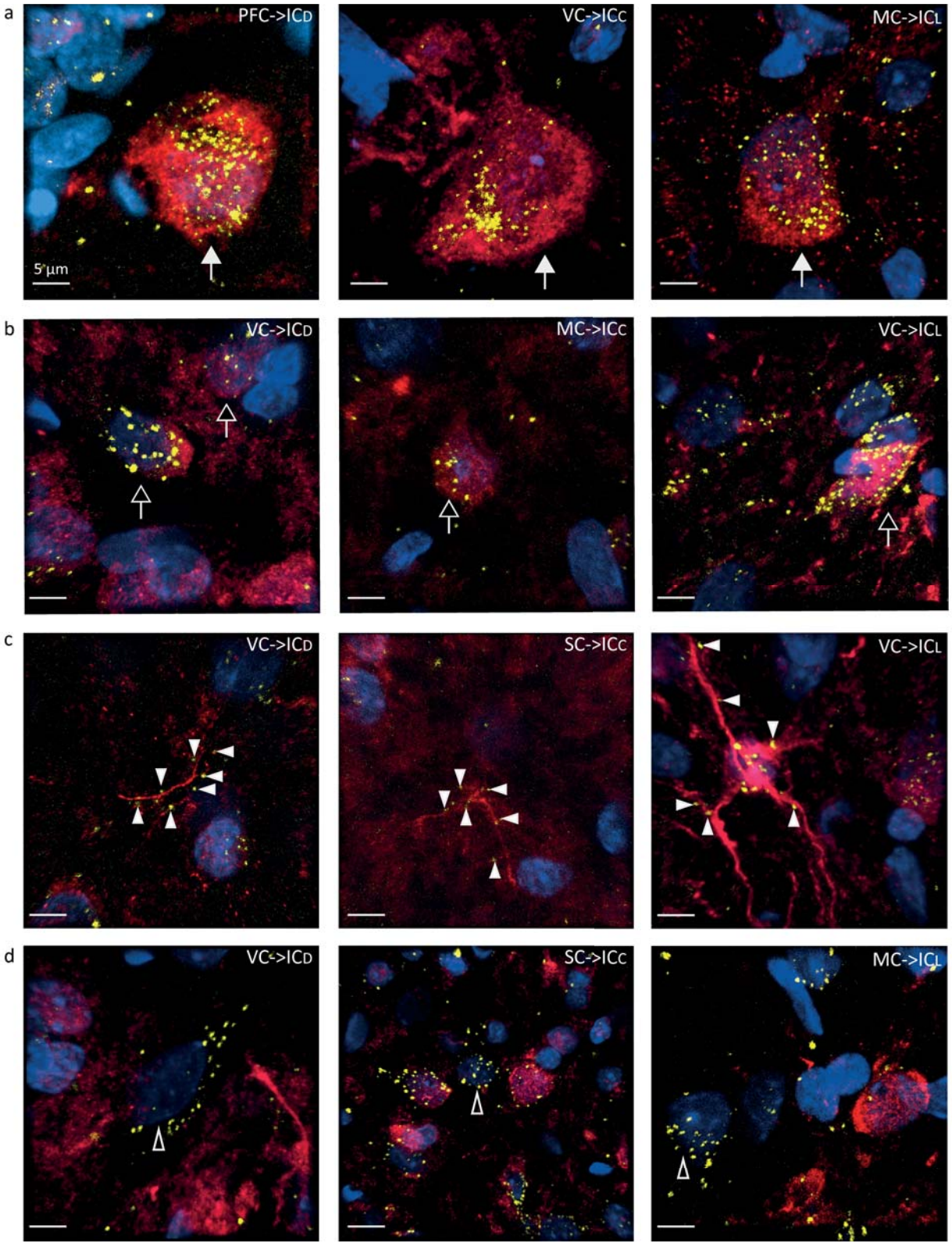
a
PFC->ICD
VC->ICC
MC->ICL
5 µm
b
VC->ICD
MC->ICC
VC->ICL
c
VC->ICD
SC->ICC
VC->ICL
d
VC->ICD
SC->ICC
MC->ICL